Rev. Roum. Sci. Techn.– Électrotechn. et Énerg.
Vol. **63**, *2*, pp. 000–000, Bucarest, 2018

Génie biomédicale

Dedicated to the memory of Academician Andrei Țugulea

THE BRACHIAL ELECTRICAL BIOIMPEDANCE AS A LOCALIZED CARDIOVASCULAR INVESTIGATION TECHNIQUE

ALEXANDRU MIHAIL MOREGA[1,2], ALIN A. DOBRE[1], MIHAELA MOREGA[1]

Key Words: Cardio-vascular electrical impedance, Brachial cardiovascular impedance (BCVI), Brachial arterial flow, Numerical modelling.

This paper aims to elicit the BCVI as a non-invasive, unobstructive method for the evaluation of cardiovascular hemodynamic indices, at the brachial (upper arm) level. A coupled mathematical model of the brachial hemodynamic flow and the electrical field, where the electrical conductivity of the arterial blood that depends on the flow characteristics is a key element, is formulated and solved numerically. Numerical simulation results suggest that BCVI information may be correlated with and used to complement the ECG and pulsometry measurements in providing a more comprehensive picture of the local and general cardio-vascular state of health.

1. INTRODUCTION

Recently, there is an increasing interest in techniques that may provide for non-invasive, affordable, readily available yet accurate information to unveil the localization, emergence, and progression of complex hemodynamic flows. Timely and consistent screening methods aimed to outline the underlying potential and acting hemodynamic factors in carotid, coronary, abdominal, and femoral arteries are of major concern. They might better portray, predict, and help infer the occurrence and progression of cardiovascular diseases that are sought of as the main contemporary cause of mortality [1,2].

Along this line, non-invasive *thoracic electrical bio-impedance* (thoracic EBI) methods are sound candidates because they provide for accurate information on cardiovascular vital parameters. Either *per se* or correlated with respiratory and *electrocardiographic* (ECG), EBI provides relevant cardio-respiratory indices that are caused by several hemodynamic factors, such as the *cardiac output* (CO), the *stroke volume* (SV), the *flow time* (FT), the *systemic vascular resistance* (SVR), etc. [3]. EBI is sensitive to the changes in the electric conductivity of the tissues, and it sums up the contribution of thoracic fluids (the thoracic blood volume), the cardiac cycle, and changes produced by respiration [2]. The dynamics of the bioimpedance resembles that of the arterial blood pressure.

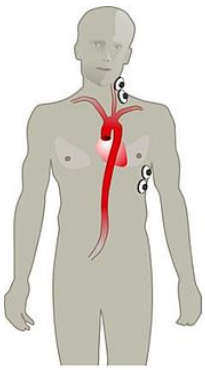

Fig. 1 – The electro-cardiometry ECM [5]. The outer pair of electrodes is used for electrical current input/output, and the inner pair of electrodes measures the voltage output.

In particular, the *impedance cardiography* (ICG) [4] and the *electro-cardiometry* (ECM) [5–7] are currently used to monitor the cardio-vascular activity through the changes in the electrical conductivity of the arterial blood. The medical application of the ECM was aimed to the general cardiac output assessment of myocardial ischemic injury [7, 8].

An array of four surface electrodes (Fig. 1) is used to input and to acquire the electrical signals: an electric current, $i(t)$, of low frequency, O(1 MHz), and amplitude, O(1 mA), conveyed by the outer electrodes, produces a voltage, $u(t)$, which is collected at the inner electrodes.

The voltage to current ratio, the bioimpedance, and its time derivative are computed on-line. The bioimpedance is associated with the *derived bioimpedance*, $\mathrm{d}Z(t) \overset{\text{def}}{=} Y(t) = 1/Z(t) = i(t)/u(t)$ (an admittance), interpreted as a measure-of-conductivity, and to its time derivative, . A mathematical model and numerical simulation results of the ECM are reported in [9].

In this paper we propose a localized version of EBI, at the arm level, the traditional place for blood pressure measurement, the BCVI, aimed to elicit EBI cardio-vascular indices at the brachial (arm) level – Fig. 2.

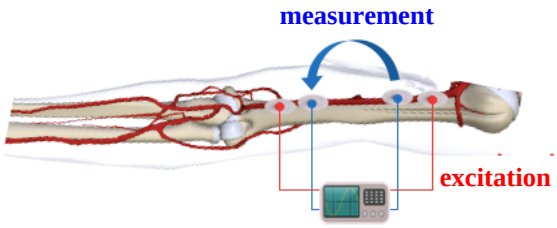

Fig. 2 – The Brachial cardiovascular impedance (BCVI) implementation.

The main reasons for this particular form of EBI are the presence and accessibility of the brachial artery, which is close to the aortic arch, and its relatively close positioning to the surface of the arm.

Although maybe not all hemodynamic flow indices might thus be available, as compared to the ECM, we may infer that BCVI may be a relevant, useful, easily accessible cardiovascular monitoring technique. Furthermore it may be complemented by the blood pressure monitoring, using a unique apparatus.

To substantiate this idea, this paper introduces a mathematical model for CVI technique, its numerical implementation, and numerical simulation results concerning the BCVI and its time derivative. Although the EBI procedure requires an ac excitation, in this first stage study

"Politehnica" [1]University of Bucharest, Romania, E-mail: amm@iem.pub.ro, alin.dobre@upb.ro, mihaela@iem.pub.ro
[2]Institute of Statistical Mathematics and Applied Mathematics "Gheorghe Mihoc – Caius Iacob", Bucharest, Romanian Academy

we use an electrokinetic mode to probe the BCVI feasibility and relevance, whereas the ac analysis is under current research.

2. THE ELECTRICAL CODUCTIVITY OF THE ARTERIAL BLOOD

The cyclic variation of the electrical conductivity of the aortic blood causes periodic changes in the shape and the orientation of the red blood cells (RBC), Fig. 3 [9]. These changes are perceived as changes in the derived bioimpedance, $dZ(t)$, and its time-derivative . They may be synchronised with pulse plethysmography signals and ECG measurements, and correlated with the changes in the cardiovascular activity, which may be quantitatively expressed through the cardiovascular indices. The sketches related to the diastolic and systolic phases signals suggest the changes in RBCs orientation due to the aortic valve flow, as cause for the variation in the electrical conductivity of the blood.

Figure 3 renders the orientation of the RBCs during the diastolic and systolic phases. In the diastolic phase the electrical conductivity is low: right before the aortic valve opens the RBCs are randomly distributed, which explains the high electrical resistivity of the blood. In the systolic phase the electrical conductivity of blood is high: the sketch at the right shows the RBCs right after the aortic valve opens. They are aligned streamwise and change their shape in response to the increase in the flow rate, which leads to the electric conductivity of the blood increase.

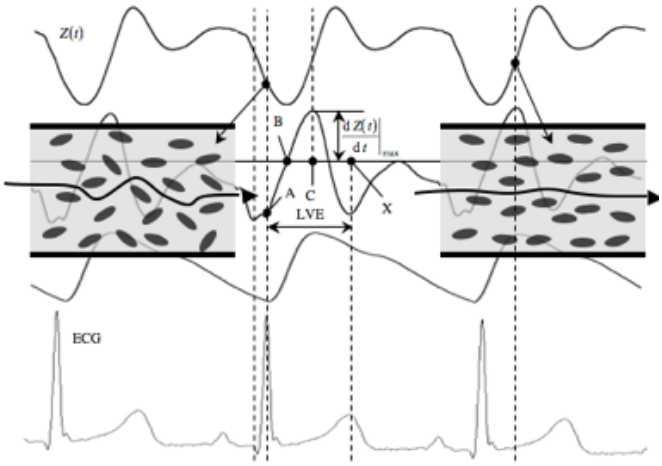

Fig. 3 – Synchronized derived bioimpedance, its time derivative, ECG, and pulse plethysmogram signals. The orientation of the RBCs in the aorta before and after the aortic valve opens (after [7]).

EBI senses the pulsatile variations of the arterial flow. A pair of dual electrodes – for electrical current input/output, and for voltage output – is used to acquire suitable data to compute the EBI signal. Its time derivative senses the dynamics of the blood electro-conductivity, which varies during the cardiac cycle due to the complex, cyclic (re)orientation of the RBCs.

The time derivative of the derived biompedance (an admittance) detects the changes in the electrical conductivity of the arterial blood during the cardiac cycle, caused by the complex interaction between the blood flow and the RBCs that produces changes in their orientation and deformation.

3. A MORE REALISTIC COMPUTATIONAL DOMAIN

In this BCVI study a more realistic human anatomical model (upper arm) with non-homogeneous structure is utilized. Starting from a set of approx. 400 high resolution MRI images of the arm), in digital imaging and communications in medicine (DICOM) format [10]. Using specialized software [11, 12], the result is the final computational domain of the upper arm presented in Fig. 4,a, which is then discretized (Fig. 4,b) and used for the numerical simulation of BCVI.

a. The arm and its inner anatomical regions, built using reconstruction technique out of DICOM sets.

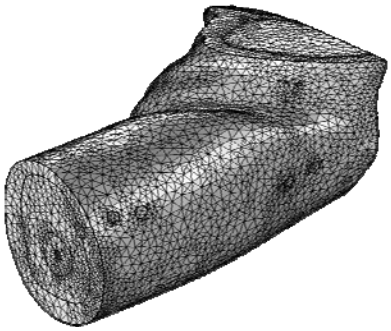

b. Finite element mesh made of appox. 130,000 Lagrange, quadratic, tetrahedral elements.

Fig. 4 – The model of the upper arm and the FEM mesh used to numerically simulate the BCVI.

Details on the numerical processing of the DICOM set may be found elsewhere, *e.g.*, [13, 14].

4. THE MATHEMATICAL MODEL OF THE BCVI

Two coupled physical phenomena occur in the BCVI problem: the pulsatile blood flow in the brachial artery and the electric field diffusion. The brachial artery wall deformation is negligibly small [15, 16] therefore a structural model is not needed actually.

The rheological model of the blood, though a complex fluid, is Newtonian, with constant properties, consistent with the assumption that the brachial artery is a relatively large vessel [9]. The brachial hemodynamic is cyclic, the flow is laminar, incompressible, and the fluid (blood) is Newtonian.

The mathematical model for "resistive" type vessels is then made of the unsteady momentum balance (Navier-Stokes) and the mass conservation law [14, 17]

$$\rho\left[\frac{\partial \boldsymbol{u}}{\partial t}+(\boldsymbol{u}\cdot\nabla)\boldsymbol{u}\right]=\nabla\left[-p\boldsymbol{I}+\eta\left(\nabla\cdot\boldsymbol{u}+(\nabla\cdot\boldsymbol{u})^{\mathrm{T}}\right)\right],\ \nabla\cdot\boldsymbol{u}=0\ ,(1)$$

where ρ = 1 050 kg/m^3 is mass density, ***u*** [m/s] the velocity field, p [Pa] the pressure field, and ***I*** is the unity matrix.

The dynamic viscosity η [Pa·s] depends on the viscosity of the plasma and on the volume of hematocrit, H, [18]

$$\eta = \eta_{pl}\left(1 + 2.5H + 7.37\times10^{-2}H\right) \tag{2}$$

Here, $\nu_{pl} = 1.35\times10^{-3}$ Pa·s. The upstream flow is modelled by an inlet cyclic, uniform boundary velocity profile that is derived from Womersley's theory – Fig. 5 [9, 19].

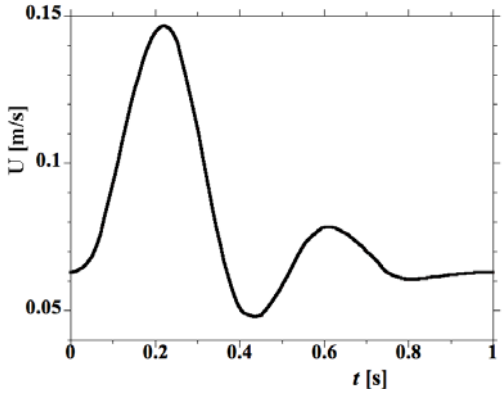

Fig. 5 — The inlet velocity profile [9].

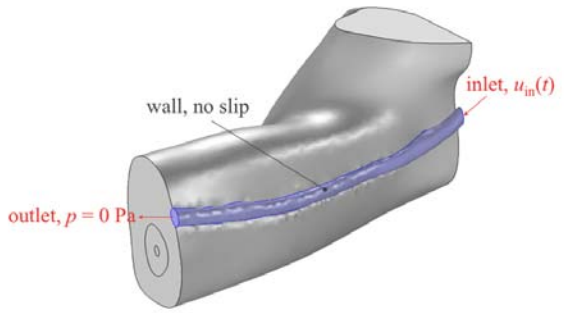

a. The hemodynamic model.

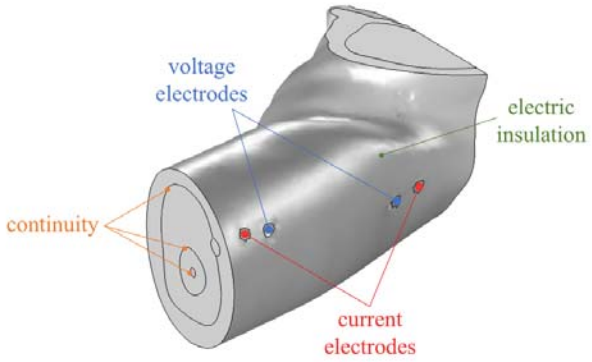

b. The electrokinetic model.

Fig. 6 — The boundary conditions that close the BCVI problem.

The mathematical model of the electric field is described by the elliptic partial differential equation [9]

$$\nabla\cdot\left(\sigma\nabla V\right) = 0\,, \tag{4}$$

where, V [V] is the electric potential. The electric current density, ***J*** [A/m^2], is given by , where σ [S/m] is the electrical conductivity.

The surface of the computational domain (the skin), is assumed electrically insulated, ***n***·***J*** = 0, where ***n*** is the outward pointing normal. The inner (voltage) pair of electrodes is modelled as floating potential surfaces, and for the outer (excitation) pair of electrodes we assume incurrent flow and ground boundary conditions, respectively. Figure 6 specifies the boundary conditions for the BCVI problem (1)-(4).

Table 1

The electrical conductivity of the different anatomic regions [20].

Tissue	**Electrical conductivity [S/m]**
Blood	0.66
Bone	0.006
Muscle	0.355
Marrow	0.00247
Arm	0.17

Table 1 lists the electrical conductivity for the main anatomic regions accounted for in this study [20].

More elaborated theories devoted to blood flow – conductivity interactions are available, e.g. [18], but they are concerned with Poiseuille-type flows, and may not model the arterial hemodynamic. In this study we use an equivalent electrical conductivity for the arterial blood, assimilating the RBCs within plasma with a dilute suspension of ellipsoidal globules, which we introduced to model the ECM [9]. The aorta is treated as an equivalent circular, straight, cylindrical tube. The dynamics of the electrical conductivity, which depends on the flow, may be modelled, as introduced in [9, 13, 14], based on [20]

$$\sigma_b = \sigma_{pl}\frac{1-H}{1+(C-1)H}\,, \tag{5}$$

where σ_b and σ_{pl} [S·m^{-1}] are the electrical conductivities of blood and plasma. C is a geometrical shape factor for the RBC, assimilated with ellipsoids of axes $a < b$, which in the circular tube theory a function of the tube radius, r_0

$$C(r_0) = f(r_0)\cdot C_b + [1 - f(r_0)]\cdot C_r\,,$$

$$C_r = (C_a + 2C_b)/3,\, C_a = 1/M\,,\, C_b = C(r_0) = 2/(2-M)\,, \tag{6}$$

where for a/b = 0.38, $M \cong a/b$. The orientation rate is approximated by

$$f(r) = \frac{n}{n_0}\frac{\theta_0^{-1}(r)}{\theta_d^{-1}(r) + \theta_0^{-1}(r)}\,, \tag{7}$$

where n is the number per unit volume of RBCs parallel to the flow (stable orientation), n_0 is the total number per unit volume of RBCs, and r is the duct radius. θ_d [s] is the time constant for cells disorientation (or cell randomization). θ_0 [s] is the cell orientation time constant (from random to aligned with the flow), which is proportional to the inverse of the shear rate. θ_d is proportional to the inverse of the square root of the shear rate θ_0.

The deformation of RBCs due to the viscous shear flow is related to the shear stress in the fluid, τ_w [N/m^2], approximated in Hagen-Poiseuille flow by the average friction factor [21]

$$\tau_w = \eta\left(-\frac{\mathrm{d}u}{\mathrm{d}r}\right)\Bigg|_{r=r_0} = 4\eta\frac{U}{r_0}\,, \tag{8}$$

Here μ [Pa·s] is the dynamic viscosity, u [m/s] is the

velocity, U [m/s] is the cross-sectional average velocity. The brachial artery in our study is reconstructed from MRI slices and it is not a straight, round tube, therefore the mathematical model (5)–(8) is not readily applicable. To solve this difficulty, we propose an *equivalent* round tube for the artery [9]:
– the tube radius, r_0, is that of the artery average cross-sectional area;
– the tube length is the ratio between the volume of the brachial artery and its average cross-sectional area;
– the average velocity, U, which is calculated using the mass flow rate.

The shear rate obtained from numerical simulation, $\tau_w > 0.1$ N/m^2, is consistent with the mathematical model of the electrical conductivity (5) predicted by [18].

5. NUMERICAL SIMULATION RESULTS AND DISCUSSION

The BCVI mathematical model (1–8) is solved numerically, by using the finite element method (FEM) [22]. The solution to the BCVI may be divided into two main steps. First, the cyclic arterial (brachial) blood flow is solved, starting from homogeneous initial conditions, until quasi-stationary state is reached, Eqs. (1) and (2).

Then, the electrical field problem is numerically integrated for each time step of the flow, for the last period of the flow problem. The cyclic electrical conductivity of the blood is computed assuming an equivalent volume for the flow, for each saved time step of the flow. Details of this approach, concerning the ECM study, may be found also in [9].

a. The hemodynamic flow – values are in m/s.

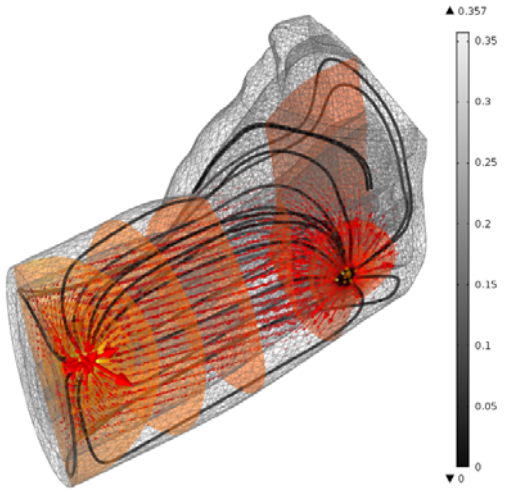

b. The electrokinetic field – values are in volts.

Fig. 7 – Numerical simulation results at t = 0.22 s, during the maximum diastolic flow rate (Fig. 5). Dimensions are in meters.

Figure 7 shows the hemodynamic flow (streamlines and arrows for the velocity, surface color map for the pressure) and the electrokinetic field (surface gray map for the voltage, equipotential surfaces, and field tubes and arrows for the electrical current density) at t = 0.22 s, about the maximum flow rate (Fig. 5).

Figure 8 presents published data on measured derived bioimpedance and its time derivative. Several remarkable vascular parameters that may be recognized are marked.

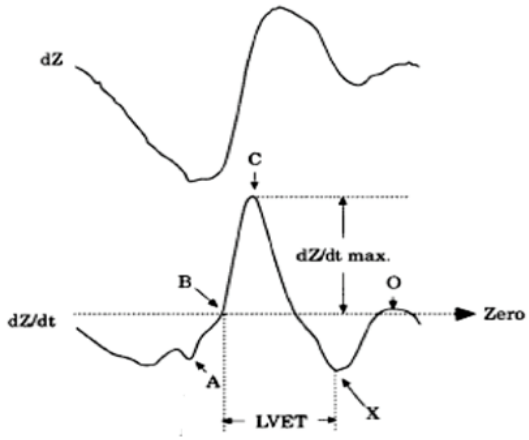

Fig. 8 – Derived (up) cardiovascular bioimpedance and its time derivative (down) [23] – experimental data.

Figure 9 gives the non-dimensional derived impedance of the brachial blood, evaluated as shown in Section 3, where $\tilde{Y} = (Y - Y_{min})/(Y_{max} - Y_{min})$. Here, Y_{max} = 8.1481 mS and Y_{min} = 8.1414 mS, obtained by numerical simulation.

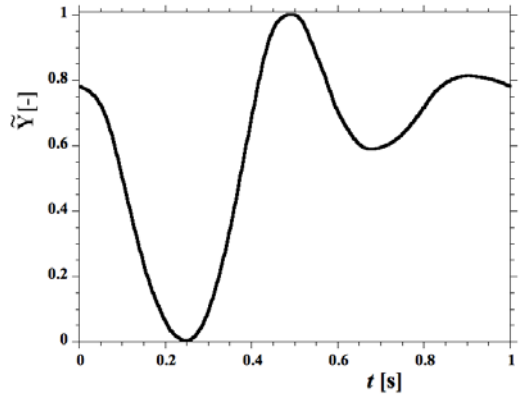

Fig. 9 – The derived BCVI, non-dimensional, numerical simulation results.

Apparently, BCVI dynamics follows the velocity profile, seen in Fig. 5. This is a new result as such reported studies and clinical investigation techniques (ECM, ICG) are concerned with aortic blood flow dynamics.

Figure 10 displays the time derivative of the BCVI and some relevant vascular indices that may be calculated by using it.

Hemodynamic events, pinpointed and detailed in [23, 24], are discernable and measurable through the numerical BCVI:

B – the start of ejection of blood by the left ventricle,
O – the diastolic upward deflection,
C – the major upward systole deflection,
LVET – the left ventricular ejection time,

X – the closure of the aortic valve,

$d(dZ)/dt_{max}$ – the maximum change in impedance during the systole phase.

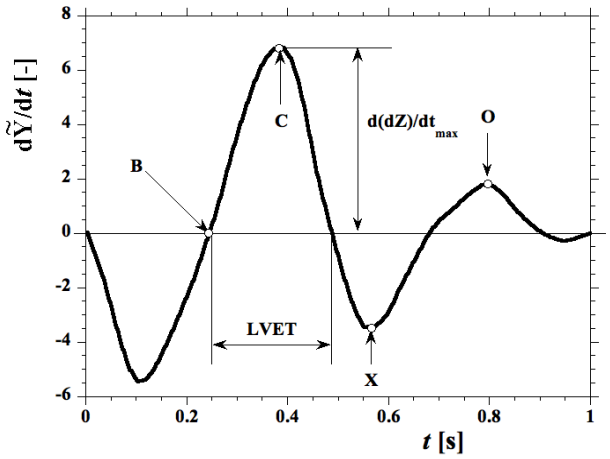

Fig. 10 – The time derivative of the BCVI, numerical simulation results.

The values of these indices may differ from those of their counterparts measured using the ECM because it seems reasonable to expect discrepancies when using impedance measurements on different arterial branches, situated farther to the heart.

On the other hand, details such as the A-wave (revealed by the ECM, experimentally (Fig. 8) and numerically [9]) are not evidenced in the numerical BCVI. It is yet to investigate experimentally if this is a limitation of the BCVI with respect to the ECM[1].

The dc (used in this study) and AC (the current working regime for the EBI) models were shown to provide for similar cardiovascular indices for the ECM EBI [9], suggesting that the first stage electrokinetic model may be used with negligible loss of accuracy within the limits of the volume conductor hypothesis (the penetration depth of the electromagnetic field is larger than the anatomical regions length scales).

6. CONCLUSIONS

This paper presents the direct problem of the brachial cardio vascular bioimpedance (BCVI), as a localized (at the upper arm level) EBI. It aims to establish a consistent mathematical model that describes the outlining physical phenomena, which may be used in numerical simulations to assess the sensitivity of BCVI and thus providing for the detection and quantification of several vascular indices specific to brachial arterial blood flow correlated with the cardiac cycle electrophysiology. It outlines also several aspects concerning the non-invasive and unobtrusive EBI evaluation in vascular cardiology.

In passing from laboratory validated experiments and analytic models to the real operational conditions of the EBI procedure a major problem is the realism and consistency of the computational domain, which is used to perform the numerical simulations. Therefore, here, a 3D realistic representation of the upper arm was constructed out of MRI images.

The usage of anatomically realistic computational domains to compute arterial flows, here brachial flow, may raise concerns in using known results on the electrical conductivity of the arterial blood. This difficulty is solved by an equivalent electrical conductivity of the arterial blood (function of flow rate), based on known analytic and experimental results. Several nonlinear electrophoresis effects (e.g., the delayed, hysteretic change of the electrical conductivity of blood for decelerating and accelerating flows), although approachable too, are not considered here, they make the object of a future research. However, the relevance of BCVI to the dynamics of the brachial arterial flow is clearly evidenced.

We assumed a dc excitation that, from the numerical simulation perspective, proves to evidence the hemodynamic of the brachial artery. The analysis of the ac regime, commonly used in EBI techniques, makes the object of a future research. However, previous work conducted on the ECM bioimpedance, *e.g.,* [9], shows off that the two BCVIs (dc and ac) provide closely related numerical results.

The derived bioimpedance and its time derivative computed from BCVI clearly evidence and provide for the quantitative assessment of several cardiac hemodynamic indices, for instance (Fig. 10): the beginning of ejection of blood by the left ventricle, the major upward systole deflection, the closure of the aortic valve, the diastolic upward deflection, the left ventricular ejection time, the maximum impedance change during systole. We point out that the values produced by BCVI might be different from those provided by the ECM or ICG. Their comparison makes the object of future experimental work.

Although maybe not all hemodynamic flow indices might thus be available, as compared to the ECM, we may infer that BCVI may be a relevant, useful, easily accessible cardiovascular monitoring technique, which may complemented by the blood pressure monitoring, using a unique apparatus.

As mentioned, the work presented here is on a direct problem of BCVI. It may enable the formulation and then the solution of an inverse BCVI problem, aimed to unveil the dynamics of arterial flow out of BCVI experimental data. This is the object of a future research.

ACKNOWLEDGEMENTS

The work was conducted in the Laboratory for Electrical Engineering for Medicine at UPB. The second author acknowledges the financial support offered by University POLITEHNICA of Bucharest, through the "Excellence Research Grants" Program, UPB – GEX 2017. Identifier: UPB-GEX2017, Ctr. No. 1 / 25.09.2017 (HEARTACT), internal number ET 02-17-03, project ID 38.

Received on March 4, 2018

REFERENCES

1. D. Mozaffarian et al., *Heart disease and stroke statistics — 2015 update: a report from the American Heart Association*, The American Heart Association Statistics Committee, and Stroke Statistics Subcommittee, 2014, DOI: 10.1161/CIR.0000000000000152.
2. *Centers for Disease Control and Protection, Heart Disease Statistics and Maps*,

[1] The right and left atria contributions to the A-wave are yet to assess. According to some sources, the A-wave is perceived as caused by contraction of the atria, but others suspect that it is produced by the back flow of blood from the atria into the central veins. It was found that the left atrium ejection might be the main cause of this wave, and the pending ejection fraction is substantially correlated to the amplitude of the A-wave [23, 24].

http://www.cdc.gov/nchs/data/nvsr/nvsr64/nvsr64_02.pdf
3. T.N. Sathyaprabha, C. Pradhan, G. Rashmi, K. Thennarasu, T.R.Raju, *Noninvasive cardiac output measurement by transthoracic electrical bioimpedence: Influence of age and gender*, J Clin Monit Comput., **22**, *6*, pp. 401–408, 2008. DOI: 10.1007/s10877-008-9148-6.
4. D.P. Bernstein, *Impedance cardiography: Pulsatile blood flow and the biophysical and electrodynamic basis for the stroke volume equations*, J Electr. Bioimp. **1**, *1*, pp. 2–17, 2010.
5. Cardiotronic, Inc. www.cardiotronic.net
6. D.P. Bernstein, M.J. Osypka, *Apparatus and method for determining an approximation of stroke volume and cardiac output of the heart*. US Patent No. 6, 511,438. http://www.google.com/patents/US6511438.
7. M. Osypka, *An Introduction to Electrical Cardiometry*. Berlin, Germany, pp. 1–10, http://www.cardiotronic.net
8. F. Mellert, K. Winkler, C. Schneider, T. Dudykevych, A. Welz, M. Osypka, E. Gersing, C.J. Preusse, *Detection of (reversible) myocardial ischemic injury by means of electrical bioimpedance*. IEEE Trans. Biomed. Eng. **58**, *6*, pp. 1511–1518, 2011. DOI: 10.1109/TBME.2010.2054090.
9. A.M. Morega, A.A. Dobre, M. Morega, *Electrical cardiometry simulation for the assessment of circulatory parameters*, Proc. of the Romanian Academy, Series A, **17**, *3*, pp. 259–266, 2016.
10. *Visible Human Project*, U.S. National Library of Medicine, National Institutes of Health http://www.nlm.nih.gov/research/visible/visible_human.html.
11. ScanIP, +FE and +CAD Reference Guide, Simpleware Ltd., UK, 2010.
12. Simpleware 4.2, Simpleware Ltd., UK, 2010.
13. A.M. Morega, A.A. Dobre, M. Morega, *Numerical simulation in electrical cardiometry*. Proc. 13th Int. Conf. on Optimization of Electrical and Electronic Equipment (OPTIM) Braşov, Romania, 2010, pp. 1407–1412.
14. A.M. Morega, A.A. Dobre, M. Morega, *Blood flow indices assessment by electrocardiometry*. in: S. Ion, C. Popa (eds.) *Topics of Mathematical Modeling of Life Sciences Problems*, MatrixRom, Bucharest, Romania, 2013, pp. 43–66.
15. A.A. Dobre, A.M. Morega, M. Morega, *The investigation of flow – structural interaction in an arterial branching by numerical simulation*. IFMBE Proc. 10th IEEE Int. Conf. Information Technology and Applications in Biomedicine (ITAB) Corfu, Greece, 2010.
16. A.M. Morega, A.A. Dobre, M. Morega, *Numerical simulation of magnetic drug targeting with flow-structural interaction in an arterial branching region of interest*, Proc. Comsol Users Conference Paris, France, pp. 17–19, 2010.
17. A.A. Dobre, A.M. Morega, M. Morega, C.M. Ipate, *Numerical simulation in electrocardiography*, Rev Roum Sci Techn – Électrotechn. et Énerg., **56**, *2*, pp. 209-218, 2011.
18. A.E. Hoetink, T.J.C. Faes, K.R. Visser, R.M. Heethaar, *On the flow dependency of the electrical conductivity of blood*, IEEE Trans. Biomed. Eng., **51**, *7*, pp. 251–1261, 2004. DOI: 10.1109/TBME.2004.827263.
19. C.A. Taylor, T.J.R. Hughes, C.K. Zarins, *Finite element modeling of three-dimensional pulsatile flow in the abdominal aorta: relevance to atherosclerosis*, Ann. Biomed. Eng., **26**, pp. 975–987, 1998.
20. R.L. Gaw, B.H. Cornish, B.J. Thomas, *The electrical impedance of pulsatile blood flowing through rigid tubes: A theoretical investigation*, IEEE Trans. on Biomed. Eng., **55**, *2*, pp. 721–727, 2008.
21. A. Bejan, *Heat Transfer*, J. Wiley & Sons Inc., New York, pp. 295–298, 1993.
22. Comsol Multiphysics, AB, v. 3.5a, 5.3a, 2010–2018.
23. J. Vedru, *Electrical impedance methods for the measurement of stroke volume in man: state of art*, Acta & Comm. Uni. Tartuensis (Jartu, Estonia) **974**, pp. 110–129, 1994. http://kodu.ut.ee/~vedru/PUB/EImet_94.pdf.
24. H.H. Woltjer, H.J. Bogaard, P.M.J.M. de Vries, *The technique of impedance cardiography*, Eur. Hear.t J., **18**, pp. 1396–1403, 1997.